Cell

Derivation of Pre-X Inactivation Human Embryonic Stem Cells under Physiological Oxygen Concentrations

Christopher J. Lengner,[1,11] Alexander A. Gimelbrant,[4,5,11] Jennifer A. Erwin,[6,7,8] Albert Wu Cheng,[1,3] Matthew G. Guenther,[1] G. Grant Welstead,[1] Raaji Alagappan,[1] Garrett M. Frampton,[1,2] Ping Xu,[1] Julien Muffat,[1] Sandro Santagata,[1] Doug Powers,[9] C. Brent Barrett,[10] Richard A. Young,[1,2] Jeannie T. Lee,[6,7,8] Rudolf Jaenisch,[1,2,*] and Maisam Mitalipova[1,*]

[1]Whitehead Institute for Biomedical Sciences, 9 Cambridge Center, Cambridge, MA 02142, USA
[2]Department of Biology
[3]Department of Computational and Systems Biology
Massachusetts Institute of Technology, Cambridge, MA 02139, USA
[4]Department of Cancer Biology, Dana Farber Cancer Institute, Boston, MA 02115, USA
[5]Department of Pathology
[6]Department of Genetics
Harvard Medical School, Boston, MA 02114, USA
[7]Department of Molecular Biology, Massachusetts General Hospital, Boston, MA 02114, USA
[8]Howard Hughes Medical Institute
[9]Incept Biosystems, Ann Arbor, MI 48108, USA
[10]Boston IVF, The Waltham Center, Waltham, MA 02451, USA
[11]These authors contributed equally to this work
*Correspondence: jaenisch@wi.mit.edu (R.J.), mitalipo@wi.mit.edu (M.M.)
DOI 10.1016/j.cell.2010.04.010

SUMMARY

The presence of two active X chromosomes (XaXa) is a hallmark of the ground state of pluripotency specific to murine embryonic stem cells (ESCs). Human ESCs (hESCs) invariably exhibit signs of X chromosome inactivation (XCI) and are considered developmentally more advanced than their murine counterparts. We describe the establishment of XaXa hESCs derived under physiological oxygen concentrations. Using these cell lines, we demonstrate that (1) differentiation of hESCs induces random XCI in a manner similar to murine ESCs, (2) chronic exposure to atmospheric oxygen is sufficient to induce irreversible XCI with minor changes of the transcriptome, (3) the Xa exhibits heavy methylation of the *XIST* promoter region, and (4) XCI is associated with demethylation and transcriptional activation of *XIST* along with H3K27-me3 deposition across the Xi. These findings indicate that the human blastocyst contains pre-X-inactivation cells and that this state is preserved in vitro through culture under physiological oxygen.

INTRODUCTION

Human embryonic stem cells (hESCs) represent a powerful tool for cell replacement therapy and tissue engineering. Established hESC lines exhibit a remarkable degree of variability with respect to their propensity to differentiate as well as their genetic and epigenetic stability. These differences have often been attributed to variable environmental conditions and culture techniques used to isolate and propagate hESCs, but the exact causes of the observed variability have been difficult to address directly due to genetic heterogeneity of hESCs confounding any comparison between different cell lines.

The state of X chromosome inactivation (XCI) can vary greatly not only between hESCs, but also between subcultures of a single hESC line (Hall et al., 2008; Shen et al., 2008; Silva et al., 2008). In mice, the paternal X chromosome is imprinted during spermatogenesis, becomes silenced during cleavage (Kalantry et al., 2009; Patrat et al., 2009), and is reactivated only in cells of the inner cell mass (ICM) of the postimplantation blastocyst while remaining silenced in the extraembryonic trophectoderm (Huynh and Lee, 2003; Mak et al., 2004; Okamoto et al., 2004; Payer and Lee, 2008). Thus, ICM-derived ESCs have two active X chromosomes (XaXa) and will randomly inactivate one X chromosome upon differentiation (XaXi) through Xist RNA coating the inactive X in *cis* (Kay et al., 1993; Monkhorst et al., 2008; Panning et al., 1997; Penny et al., 1996). Xist-mediated X chromosome silencing is accompanied by repressive histone modifications (Boggs et al., 2002; Heard et al., 2001; Kohlmaier et al., 2004; Mermoud et al., 2002; Plath et al., 2003).

Unlike mouse ESCs, all human ESC lines analyzed to date exhibit partial or complete XCI. Many of these lines lack XIST coating on the inactive X (Xi) in the undifferentiated state and do not reactivate *XIST* gene expression upon differentiation (Hall et al., 2008; Shen et al., 2008; Silva et al., 2008). Strikingly,

Table 1. hESC Derivation in Physiological O_2

					hESCs		Differentiated Cells	
Line	Isolation Date	Passage	Sex	Xi Status	XIST Expression	X-Linked Gene Expression	XIST Expression	X-Linked Gene Expression
WIBR1-5%	6/19/07	77	Male	XaY	–	NA	–	NA
WIBR1-20%	6/21/07	83	Male	XaY	–	NA	–	NA
WIBR2-5%	8/9/07	34	Female	XaXa	–	biallelic	+	biallelic
WIBR2-20%	8/11/07	54	Female	XaXi	–	monoallelic	–	monoallelic
WIBR3-5%	6/3/08	68	Female	XaXa	–	biallelic	+	biallelic
WIBR3-20%	6/5/08	60	Female	XaXi	+	monoallelic	+	monoallelic
WIBR4-5%	9/11/09	14	Female	XaXa	–	ND	+	ND
WIBR4-20%	9/18/09	12	Female	XaXi	+	ND	+	ND
WIBR5-5%	9/11/09	11	Female	XaXi	+	ND	+	ND
WIBR5-20%	9/18/09	11	Female	XaXi	+	ND	+	ND
WIBR6-5%	9/11/09	9	Male	XaY	–	NA	–	NA
WIBR6-20%	9/18/09	8	Male	XaY	–	NA	–	NA

Six hESC lines were derived under 5% O_2. WIBR1, 2, and 3 were derived from eight-cell embryos cultured until the blastocyst stage under 5% O_2. WIBR4, 5, and 6 were derived from cryopreserved blastocysts that had been cultured at 20% O_2 prior to hESC derivation in 5% O_2. (See also Figures S1, S2, and S3 for validation of pluripotency and karyotype of hESCs and Table S1 for a complete description of all human embryos used for derivation.) ND, not determined; NA, not applicable.

hESC cultures exhibit monoallelic expression of X-linked genes, suggesting that XCI in hESCs may have resulted from a nonrandom parental allele specific choice (Shen et al., 2008). However, adult females exhibit random XCI and evidence for imprinted XCI in human extraembryonic tissue is controversial (Payer and Lee, 2008). Conversely, random XCI may occur in the ICM of female embryos followed by clonal selection after hESC derivation. Staining of preimplantation female human embryos has shown that at the eight-cell stage XIST foci begin to form and expand to full XIST clouds by the morula and blastocyst stages, consistent with XCI having already occurred at this stage (van den Berg et al., 2009).

In the current study, we examine the intrinsic effects of atmospheric oxygen (~20%, pO_2, 142 mm Hg) on the ability of hESCs to maintain pluripotency, genetic, and epigenetic stability. ESC derivation and maintenance in culture is conventionally performed in atmospheric O_2 concentrations (Cowan et al., 2004; Reubinoff et al., 2000; Thomson et al., 1998), which are hyperoxic when compared to physiological O_2 levels (Fischer and Bavister, 1993). Exposure to 20% O_2 results in premature senescence and accumulation of oxidative DNA lesions (Parrinello et al., 2003) and it is possible that the hyperoxic conditions used for ESC culture have detrimental effects on cell viability and epigenetic state. Numerous reports have described protective effects of decreasing the O_2 concentrations on hESCs originally derived and maintained in atmospheric O_2 to more physiological levels such as decreased accumulation of chromosomal abnormalities (Forsyth et al., 2006), protection against spontaneous differentiation, enhanced efficiency of cloning (Ezashi et al., 2005; Forsyth et al., 2008; Ludwig et al., 2006; Prasad et al., 2009), and direct epigenetic reprogramming (Yoshida et al., 2009). Nonetheless, these findings remain controversial as recent studies called into question the beneficial effects of returning hESC lines established in atmospheric O_2 to 5% O_2 (Chen et al., 2009).

Further evidence supporting the use of physiological O_2 for the derivation and maintenance of hESCs comes from studies on preimplantation development and ESC derivation in nonhuman mammals. Exposure to atmospheric O_2 has detrimental effects on blastocyst formation rates and on cell proliferation within individual blastocysts. This was observed across many species, including mouse (Harlow and Quinn, 1979; Quinn and Harlow, 1978; Wang et al., 2006), sheep and cow (Thompson et al., 1990), goat (Batt et al., 1991; Bernardi et al., 1996), and pig (Karja et al., 2004; Kikuchi et al., 2002; Kitagawa et al., 2004). To date, such studies have not been performed with human embryos.

We demonstrate here that derivation and culture in physiological O_2 (~5%, pO_2, 36 mm Hg) aids in maintaining pluripotency and suppressing spontaneous differentiation of hESCs. Strikingly, the derivation and maintenance of hESC cultures in 5% O_2 prevented precocious XCI, suggesting that physiological O_2 helps to maintain hESCs in a more developmentally immature state.

RESULTS

Derivation of Pluripotent hESCs in a Physiological Oxygen Environment

IVF-derived eight-cell embryos were thawed and cultured in 5% O_2 until the blastocyst stage prior to hESC derivation in 5% or 20% O_2 (Table S1 available online). We established three hESC lines under 5% O_2 (designated WIBR1, 2, and 3; Figure S1) and one line under 20% O_2 (data not shown). Immediately after stable establishment, each hESC line was split at the first passage, with one half remaining at 5% O_2 and the other shifted to culture in 20% O_2. The resulting three pairs of genetically identical hESC lines were cultured for prolonged periods (>18 months, Table 1). Three additional hESC lines were derived from cryopreserved blastocysts and will be described later (Table 1).

All three pairs of cell lines maintained genetic stability, exhibited normal karyotypes (Figure S2), and expressed the pluripotency markers OCT4, SOX2, and NANOG, as well as the hESC surface markers SSEA4 and TRA1-60, at both 5% and 20% O_2 (Figure S1). All hESC lines were pluripotent as shown by teratoma formation and expression of lineage-specific transcripts during embryoid body formation (Figure S3).

Gene Expression Changes Induced by Atmospheric Oxygen

To assess changes in gene expression induced by hyperoxic culture, we analyzed the transcriptome of hESCs after acute (72 hr) or chronic exposure to 20% O_2 and compared the transcriptional profiles to hESCs maintained in 5% O_2. Acute exposure to 20% O_2 induced a dramatic change in global gene expression and resulted in a marked downregulation of genes associated with hypoxia and the HIF pathway (Figure 1A). Many of these changes were not maintained and approached baseline (5%) levels after chronic exposure to 20% O_2 (Figure 1A). Consistent with these observations, hierarchical clustering revealed that under either chronic 20% or 5% O_2 culture conditions, gene expression profiles clustered on the basis of the genetic background of the hESCs rather than O_2 environment (Figure 1B). We identified 198 genes whose change in expression after acute exposure to 20% O_2 was maintained during chronic culture (Figure S4 and Table S2). Gene set enrichment analysis across the three cell lines identified an upregulation of gene sets associated with mitochondrial activity and messenger RNA (mRNA) processing after acute exposure to 20% O_2 (Figure S4). Gene sets associated with hypoxia such as the HIF, glycolysis, and gluconeogenesis pathways were downregulated in response to both acute and chronic exposure to 20% O_2 (Figure S4).

Gene expression analysis of embryonic stem cell and lineage-specific transcripts revealed no significant changes in the expression of the core pluripotency genes OCT4, SOX2, and NANOG, whereas induction of neurectodermal, trophoblast, mesoderm, extraembryonic endoderm, and visceral endoderm genes was observed in hESCs after chronic exposure to 20% O_2 (Figure S4). This suggests that the exposure to 20% O_2 does not significantly compromise pluripotency but may promote differentiation in a fraction of the cells.

Predisposition for Spontaneous Differentiation

We tested whether atmospheric O_2 would increase the susceptibility of hESCs to undergo spontaneous differentiation under suboptimal culture conditions. We therefore cultured hESCs on mouse embryonic fibroblasts (MEFs) constitutively expressing green fluorescent protein (GFP) for 8 days without passaging, thereby triggering spontaneous differentiation. We found that the proportion of cells in the culture expressing SSEA4 and OCT4 was reduced in lines WIBR1 and WIBR2 after acute (72 hr) as well as chronic exposure to 20% O_2 (Figure 1C). In contrast WIBR3 remained largely unaffected, with over 90% of cells maintaining OCT4 immunoreactivity under all culture conditions (Figure 1C). This finding highlights the variability of hESC lines in their response to atmospheric O_2 and may provide an explanation for the conflicting reports in the literature.

Effects of Oxygen Tension on Epigenetic Stability in hESCs

To evaluate the consequences of exposure to 20% O_2 on the epigenetic stability of hESCs, we assessed the DNA methylation status of several imprinted genes using Sequenom matrix-assisted laser desorption/ionization time of flight (MALDI-TOF) mass spectrometry analysis of bisulfite modified DNA, and we observed no significant differences in methylation between 5% or 20% O_2 cultures at the DLX5, H19, KCNQ1, NDN, PLAG1, SLC22A18, and SNURF loci (data not shown). One exception was observed at the PEG3 locus, where chronic exposure to 20% O_2 was associated with increased CpG methylation. We conclude that the DNA methylation status at numerous imprinted loci remains stable in hESCs cultured in both atmospheric and physiological O_2.

We next assessed the status of XCI in the two female lines WIBR2 and 3. This is of particular interest since hESCs are similar to murine EpiSCs (Brons et al., 2007; Tesar et al., 2007) but, unlike murine ESCs, have invariably undergone XCI in most or all cells within a culture (Hall et al., 2008; Shen et al., 2008; Silva et al., 2008), consistent with the hypothesis that hESCs may not be developmentally equivalent to ICM-derived murine ESCs but rather may correspond to the more mature, post-XCI epiblast-derived EpiSCs (Guo et al., 2009; Nichols and Smith, 2009). Alternatively, cells of the human ICM, unlike the mouse, may have already undergone XCI (van den Berg et al., 2009).

To assess the status of XCI in hESCs, we used fluorescent in situ hybridization (FISH) to visualize XIST RNA. Both $WIBR2^{5\%}$ and $WIBR3^{5\%}$ exhibited no XIST-positive cells and no detectible *XIST* gene expression (Figures 2A and 2B and Figure S5). Since established hESC lines are known to irreversibly silence *XIST* after undergoing XCI, we tested the ability of $WIBR2^{5\%}$ and $WIBR3^{5\%}$ to activate *XIST* upon differentiation. In contrast to established hESCs cultured under 20% O_2, both $WIBR2^{5\%}$ and $WIBR3^{5\%}$ activated *XIST* gene expression and formed an XIST cloud on the Xi upon differentiation, indicating that these hESCs have two active X chromosomes. The XaXa status of these cells was further confirmed by performance of FISH for X-linked transcripts revealing two foci in cells cultured at 5% O_2 (Figure S6).

In contrast to cell lines maintained at 5% O_2, $WIBR3^{20\%}$ expressed high levels of XIST RNA and had XIST clouds coating the Xi in 67% of cells, with the remaining cells undergoing XCI upon differentiation (Figures 2A and 2B). X chromosome DNA FISH confirmed that these cells contained two X chromosomes in both 5% and 20% O_2 and had XIST RNA coating the full X chromosome territory at 20% O_2 (Figure S6). Furthermore, FISH for X-linked transcripts showed a single focus in cells cultured at 20% O_2, consistent with these cells having one inactivated X chromosome (Figure S6). This demonstrates that cells cultured in 20% O_2 had undergone precocious XCI, as has previously been observed in established hESC lines. $WIBR2^{20\%}$ did not exhibit *XIST* expression or XIST clouds and did not activate *XIST* upon differentiation (Figure S5), suggesting that this line is defective in XCI as has been observed previously in some established hESC lines.

To correlate XCI status and *XIST* expression with methylation of the *XIST* promoter, we performed Sequenom matrix-assisted

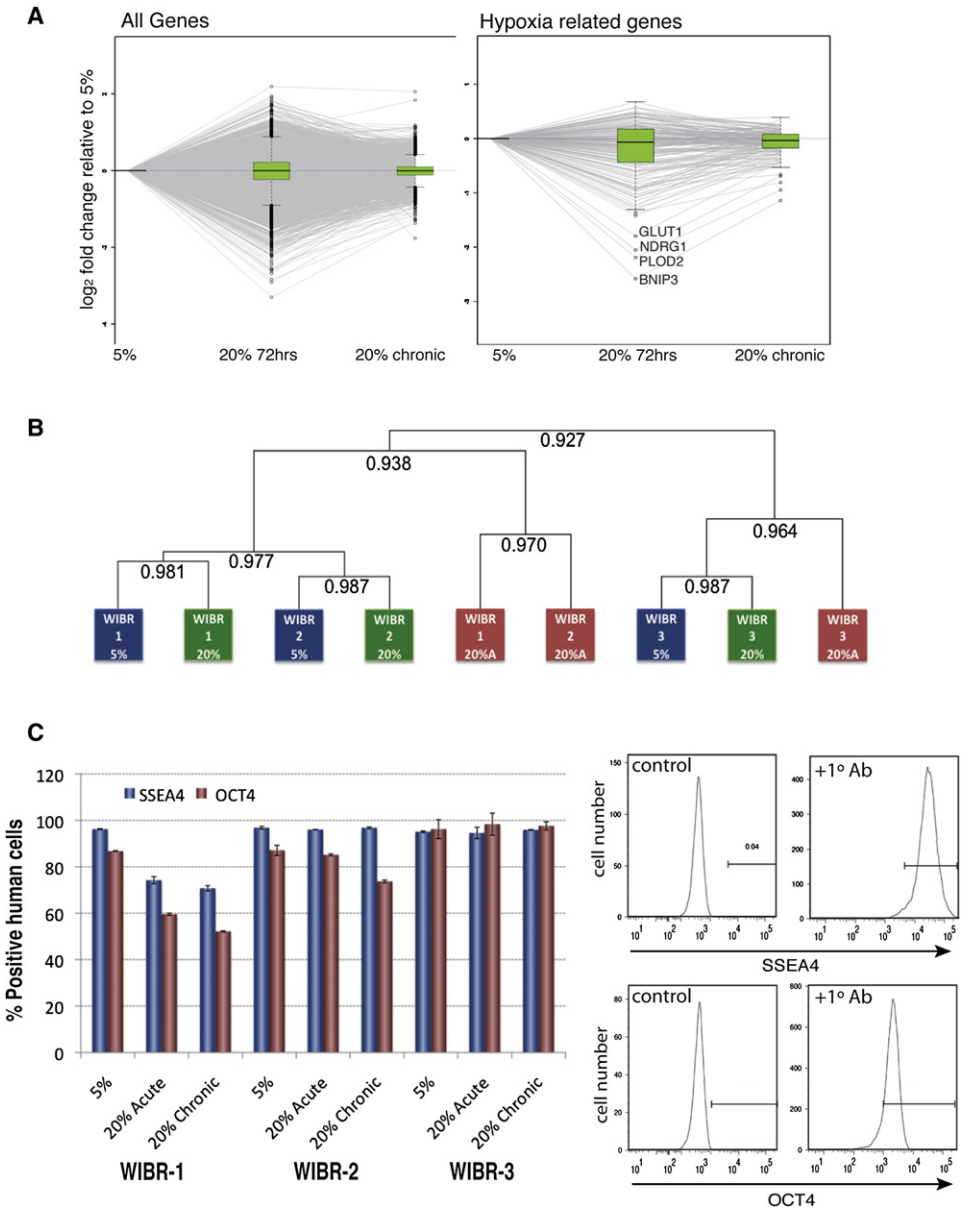

Figure 1. Effects of Atmospheric O_2 Exposure on hESC Gene Expression

(A) Changes in global gene expression and hypoxia-related gene expression after acute (72 hr) and chronic exposure to 20% O_2. Plots represent average changes across hESC lines WIBR1, WIBR2, and WIBR3. (See also Figure S4 for detailed analysis of gene expression changes and Table S2 for the list of transcripts whose change in expression was maintained after both acute and chronic exposure to 20% O_2.)

(B) Hierarchical clustering of hESC lines maintained in 5% O_2, 20% O_2, or 5% followed by 72 hr acute exposure to 20% O_2 (20A). All edges have AU p value of 100%, demonstrating that the clusters are strongly supported by the data. (Shown on the branches are the pearson correlations.) Blue boxes represent chronic 5% O_2 cultures, green boxes represent chronic 20% O_2 cultures, and red boxes represent cultures acutely shifted from 5% to 20% O_2 for 72 hr.

(C) Flow-cytometric analysis for expression of intracellular OCT4 and extracellular SSE4 in hESCs cultured in 5% O_2, 20% O_2 (chronic), or 5% followed by 72 hr exposure to 20% O_2 (acute), plotted as percent of positive human cells within the gates shown on right, after gating out GFP-positive feeders. Data are represented as the average of tree experiments ± standard deviation (SD). Representative histograms in right panels (shown for WIBR1 5%) show the gating used to quantify OCT4 and SSEA4 immunoreactivity in the absence of primary antibody (control) or in the presence of primary and secondary antibodies (+1° Ab).

MALDI-TOF mass spectrometry analysis of bisulfite-modified DNA containing two CpG islands around the *XIST* transcriptional start site. The *XIST* promoter in the male line WIBR1 as well as in female lines WIBR2$^{5\%}$ and WIBR3$^{5\%}$ exhibited over 90% methylation (Figures 2C and 2D and Figure S5). The high level of methylation at the *XIST* promoter in undifferentiated female hESCs is consistent with their lack of *XIST* expression. In contrast, female murine ESCs have only partially methylated *Xist* regulatory regions (approximately 50% on each of the two alleles) (Nesterova et al., 2008; Sun et al., 2006).

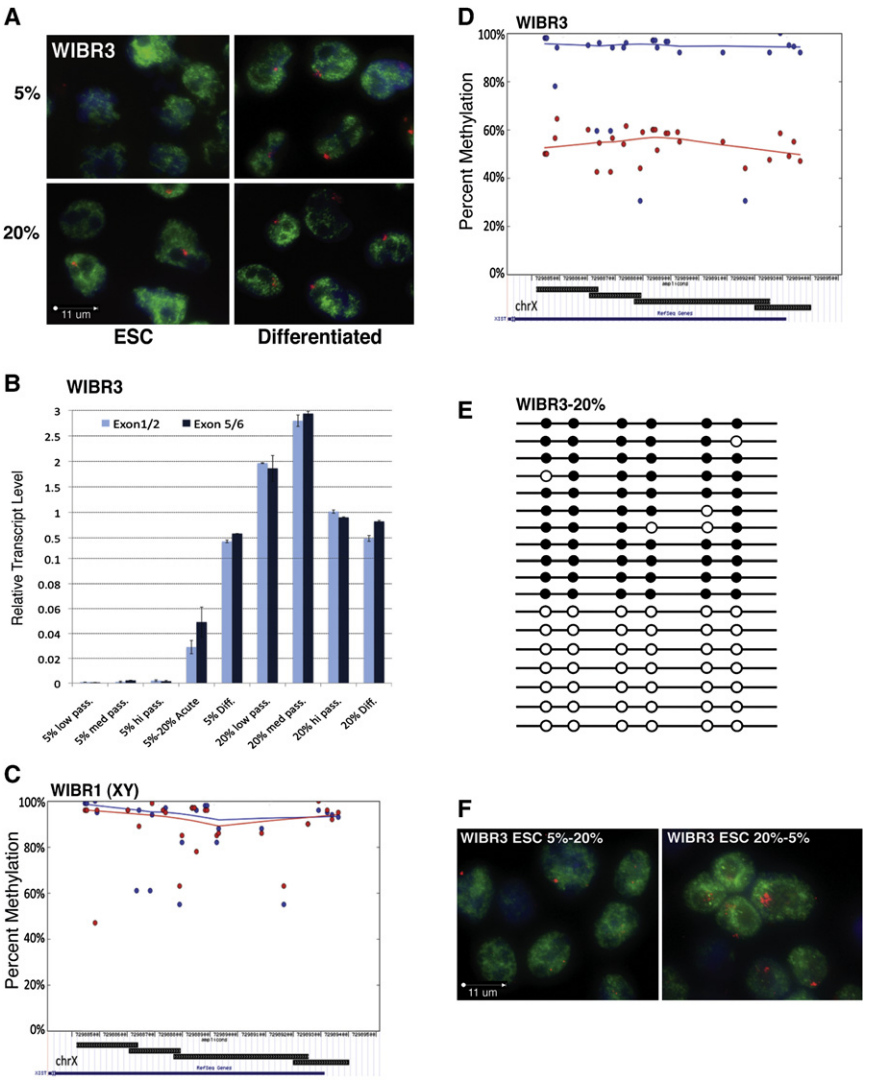

Figure 2. X Chromosome Inactivation in hESCs

(A) Epifluorescence analysis of WIBR3 hESCs and their differentiated counterparts for XIST RNA (red), CotI nuclear RNA (green), and DNA (blue) in chronic 5% and 20% O_2 cultures. (See also Figure S5 for XCI analysis of WIBR2 and Figure S6 for DNA FISH and X-linked gene FISH for WIBR3.)

(B) qRT-PCR analysis of XIST transcripts detecting two distinct exon-exon boundaries in hESCs maintained in 5% or 20% O_2 at low (<20), medium (20–40), and high (>50) passages. Also shown are XIST levels after hESC differentiation in 5% (5%-Diff) and 20% (20%-Diff) oxygen, as well as after 72 hr exposure to 20% O_2 after chronic culture at 5% O_2 (5%–20% Acute). *XIST* transcript level is normalized to GAPDH, ± SD.

(C and D) Sequenom methylation analysis of CpG islands within the *XIST* promoter/enhancer region in the male hESC line WIBR1 (C) and the female line WIBR3 (D). Five percent O_2 cultures are in blue and 20% O_2 in red. The location of the amplicons is plotted at the bottom of each graph with the gene annotation. The individual CpG residues are plotted relative to the *XIST* transcriptional start site.

(E) Bisulfite sequencing analysis of six CpG sites in single clones of the second (from the left) *XIST* promoter amplicon represented in (C) and (D).

(F) Epifluorescence analysis of WIBR3 hESCs for XIST RNA (red), CotI nuclear RNA (green), and DNA (blue) in cultures switched either from 5% to 20% O_2 or 20% to 5% O_2 for 2 weeks.

XIST promoter methylation was reduced to 50%–60% in line WIBR3$^{20\%}$ (Figure 2D). Bisulfite conversion and sequencing of individual clones revealed that the promoter was either completely unmethylated or heavily methylated, indicating that this cell line has one active *XIST* allele (Figure 2E). Line WIBR2$^{20\%}$, which exhibited no *XIST* foci and was unable to activate *XIST* expression upon differentiation, had an intermediate level of methylation, possibly reflecting earlier *XIST* activation and XCI which was subsequently followed by *XIST* gene silencing (Figure S5). To address this possibility, we performed FISH at the earliest passage of WIBR$^{20\%}$ from which enough material was available, and we found XIST foci in nearly all cells, confirming that XCI had occurred during early passages and was followed by silencing of *XIST* expression and loss of XIST clouds on the Xi during prolonged culture (Figure S5).

Allele-Specific Expression of X-Linked Genes

X-linked single-nucleotide polymorphisms (SNPs) were identified in WIBR2 and WIBR3 to measure allele-specific gene expression with SNP-Chip and Sequenom mass spectometry-based expression analyses. Initial SNP-Chip analyses of WIBR2 and WIBR3 revealed biallelic expression of nearly all X-linked SNPs in 5% O_2 cultures, consistent with these lines carrying two active X chromosomes (XaXa) (Figure 3A and Figure S7). Under 20% O_2, however, WIBR2$^{20\%}$ exhibited monoallelic expression at 31% of the SNPs (14/45), providing further evidence that this line, while lacking persistent XIST foci, underwent XCI (Figure S7). WIBR3$^{20\%}$ exhibited monoallelic expression at 73% of X-linked SNPs (with SNPs exhibiting biallelic expression lying primarily in the pseudoautosomal region known to escape XCI; Figure 3B), consistent with this line having undergone XCI.

Further quantification of allele-specific gene expression via Sequenom analysis demonstrated that both WIBR2$^{5\%}$ and WIBR3$^{5\%}$ expressed equal levels of transcript from both X chromosomes (Figure 3C and Figure S7). Line WIBR3$^{20\%}$ (XaXi and XIST positive) exhibited nearly complete monoallelic expression of the X-linked genes examined (Figure 3D). In contrast, WIBR2$^{20\%}$ (XaXi, but lacking XIST foci) expressed the majority of X-linked transcripts from a single allele. However, significant transcripts were detected from the putative Xi, suggesting that the lack of *XIST* expression and loss of XIST clouds may have resulted in a partial derepression of genes on the Xi (Figure S7).

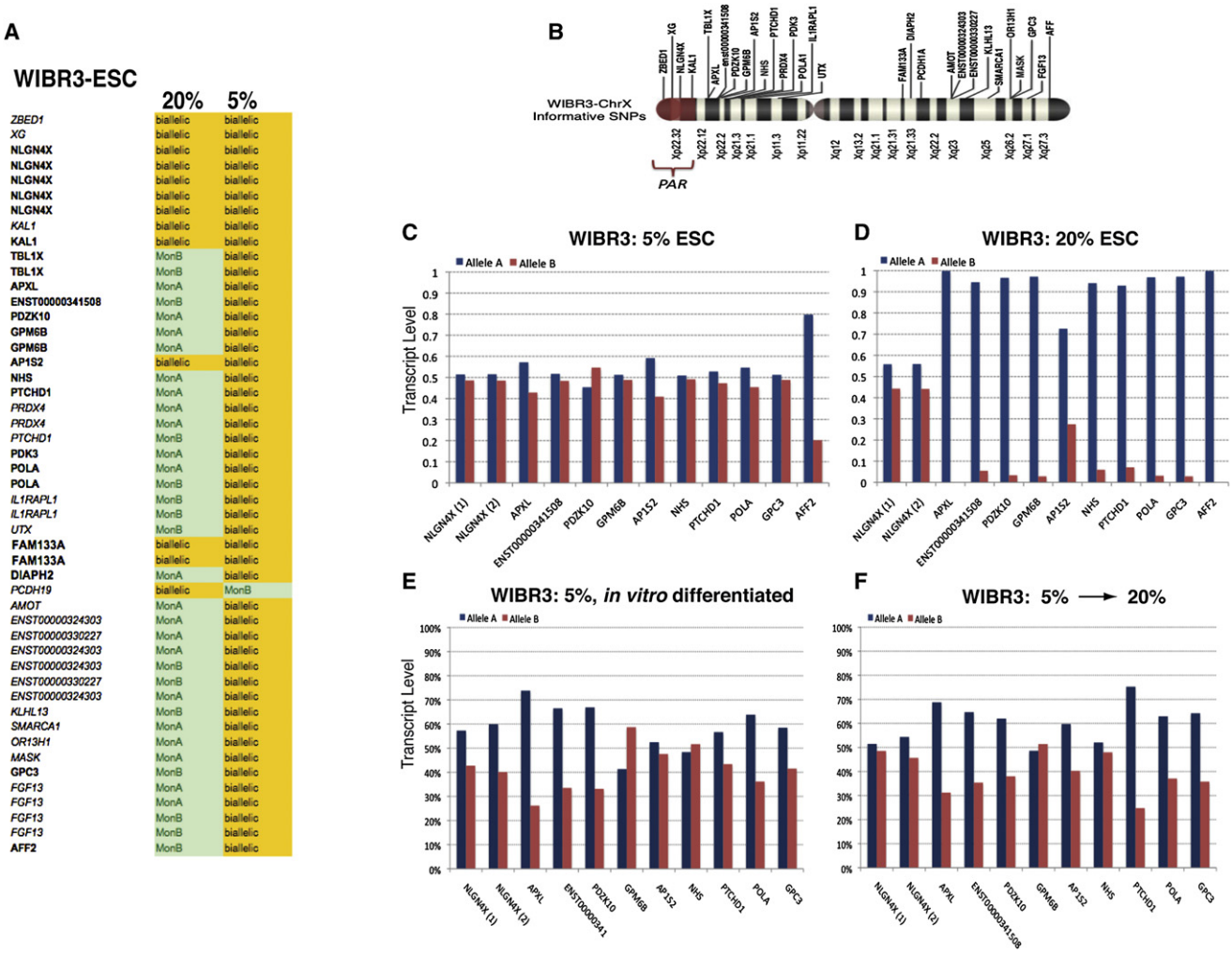

Figure 3. Allele-Specific Gene Expression in WIBR3 hESCs

(A) SNP-Chip analysis performed with all informative X-linked SNPs identified in WIBR3 hESCs. Genes are listed in order of their location relative to the pseudoautosomal region (top of the list). Genes listed are those in closest proximity to identified SNPs, with genes represented by several SNPs listed more than once. Monoallelic gene expression is denoted in green while biallelic expression is denoted in yellow.

(B) Schematic of the X chromosome displaying genes containing informative SNPs in line WIBR3 used for allele-specific expression analyses. The pseudoautosomal region (PAR) is shown in red.

(C–F) Sequenom allele-specific gene expression analysis utilizing SNPs within transcribed regions of X-linked genes (intronic and exonic) in WIBR3$^{5\%}$ ESCs (C), WIBR3$^{20\%}$ ESCs (D), WIBR3$^{5\%}$ ESCs after in vitro differentiation (E), or WIBR3$^{5\%}$ ESCs after 2 weeks of exposure to 20% O_2 (F). Genes are plotted based on their location along the X chromosome. (See also Figure S7 for allele-specific expression analysis in WIBR2.)

The monoallelic X-linked gene expression observed in established hESC cultures could be explained by precocious XCI induced under 20% O_2 culture followed by clonal selection of some cells. We directly tested whether hESCs undergo random XCI by differentiating WIBR3$^{5\%}$ in vitro for 2 weeks, a period of time long enough for cells to undergo XCI (Figure 2A) but short enough that there would not be sufficient cell division for cells to undergo clonal selection. We readily detected transcripts originating from both X chromosomes after differentiation, confirming that hESCs undergo random XCI in a manner analogous to murine ESCs (Figure 3E). This finding is consistent with the notion that the monoallelic X-linked gene expression observed in long-term cultures of XaXi hESCs is a result of clonal selection.

X Inactivation in Response to Oxidative Stress

To determine whether XCI in female hESCs cultured in 20% O_2 is reversible and whether exposure to 20% O_2 was sufficient to induce silencing of the X chromosome, we analyzed WIBR2 and WIBR3 cultures that were switched from either 5% to 20% O_2 or 20% to 5% O_2 for 2 weeks. Both WIBR2 and WIBR3 cells began to upregulate *XIST* expression and initiated the formation of XIST foci after switching to 20% O_2 (Figures 2B and 2F and Figure S5), and there were often two small XIST foci that formed indicating that these cells had not yet committed to permanent silencing of one particular X chromosome (Panning et al., 1997). Conversely, shifting of cells maintained in 20% O_2 to 5% O_2 did not reverse the established Xi in WIBR3$^{20\%}$ (Figure 2F) and had

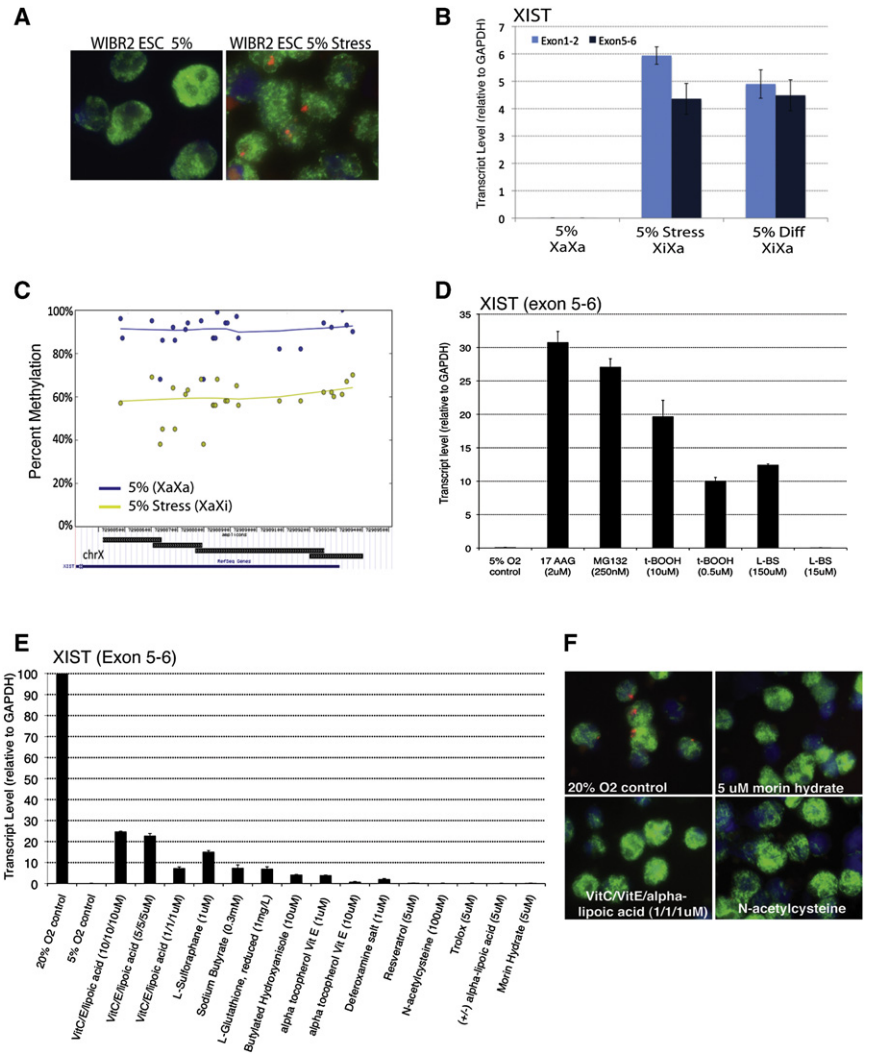

Figure 4. XCI in Response to Cellular Stress and Inhibition of XCI with Antioxidants

(A) Epifluorescence analysis of WIBR2 hESCs maintained in 5% O_2 before and after undergoing stress from a freeze-thaw cycle. XIST RNA (red), CotI nuclear RNA (green), and DNA (blue).

(B) qRT-PCR analysis of *XIST* transcripts detecting two distinct exon-exon boundaries in hESCs maintained in 5% or 20% O_2, and after freeze-thaw induced stress at 5% O_2. *XIST* transcript level is normalized to GAPDH, ± SD.

(C) Sequenom methylation analysis of CpG islands in the *XIST* promoter/enhancer region of the line WIBR2 after undergoing freeze-thaw associated stress. XaXa 5% O_2 cultures are in blue and 5% O_2 stressed XaXi cultures in yellow. The location of the CpG residues is plotted relative to the *XIST* transcriptional start site at the bottom of each graph.

(D) qRT-PCR analysis of *XIST* transcripts in WIBR2$^{5\%}$ in the absence (control) or presence of compounds inducing cellular stress (see also Table S3): HSP90 inhibitor 17AAG (24 hr acute treatment), proteosome inhibitor MG132 (24 hr acute treatment), organic peroxide tert-butyl hydroperoxide (t-BOOH, 10 μM acute treatment and 0.5 μM chronic treatment), and the γ-glutamylcysteine synthetase inhibitor L-Buthionine-sulfoximine (L-BS, 150 μM acute treatment or 15 μM chronic treatment). *XIST* transcript level is normalized to GAPDH and plotted as percent expression relative to 20% O_2, ± SD.

(E) qRT-PCR analysis of *XIST* transcripts in hESC line WIBR2 24 days after shifting of cultures from 5% to 20% O_2, during which the indicated antioxidant compounds were added to the culture media daily. Five percent control represents hESCs not shifted to 20% O_2, and 20% control represents untreated hESCs shifted from 5% to 20% O_2. *XIST* transcript level is normalized to GAPDH and expression in 20% O_2 cultures set to 100, ± SD. (See also Table S3 for a detailed description of compound concentration and use).

(F) Epifluorescence FISH analysis of representative cultures analyzed in (E). XIST RNA (red), CotI nuclear RNA (green), and DNA (blue).

no effect on WIBR2$^{20\%}$ (Figure S5). Allele-specific expression analysis of WIBR3$^{5\%}$ after 2 weeks of exposure to 20% O_2 showed biallelic expression of X-linked transcripts, consistent with random XCI (Figure 3F). These findings demonstrate that exposure to atmospheric O_2 alone is sufficient to drive irreversible X chromosome inactivation in hESCs.

In addition to atmospheric O_2 exposure, we observed promiscuous XCI in response to cellular stress induced by harsh freeze-thaw cycles in which few hESC colonies were recovered. One particular thawing of WIBR2$^{5\%}$ that resulted in low cell viability (only two to three hESC colonies recovered) exhibited XCI with XIST foci in almost all cells, high *XIST* expression, and demethylation of the *XIST* promoter (Figures 4A–4C). We therefore examined whether a general cellular stress response was sufficient to induce *XIST* activity by culturing the XaXa hESC line WIBR2$^{5\%}$ in the presence of a variety of cellular stress-inducing compounds. We found that inhibition of the proteosome, HSP90, gamma-glutamylcysteine synthetase, and treatment with organic peroxide all activated *XIST* gene expression under 5% O_2 (Figure 4D and Table S3). Thus, the XaXa state of hESCs is precarious and prone to XCI in response to cellular stress.

Antioxidant-Mediated Protection against XCI

Given that both exposure to 20% O_2 and induction of oxidative stress with organic peroxides is sufficient to drive XCI, we reasoned that addition of antioxidants to the culture media might protect against XCI. We therefore added a number of known antioxidants, a HIF1α stabilizer (because HIF pathway suppression was observed in 20% O_2; Figure 1A and Figure S4), and histone deacetylase inhibitors (because HDAC inhibition is known to suppress *XIST* expression in hESCs [Ware et al., 2009]) to WIBR2 cells cultured in 5% O_2 prior to exposure to 20% O_2 (Table S3). Twenty-four days after shifting of cultures to 20% O_2, almost all of these compounds were

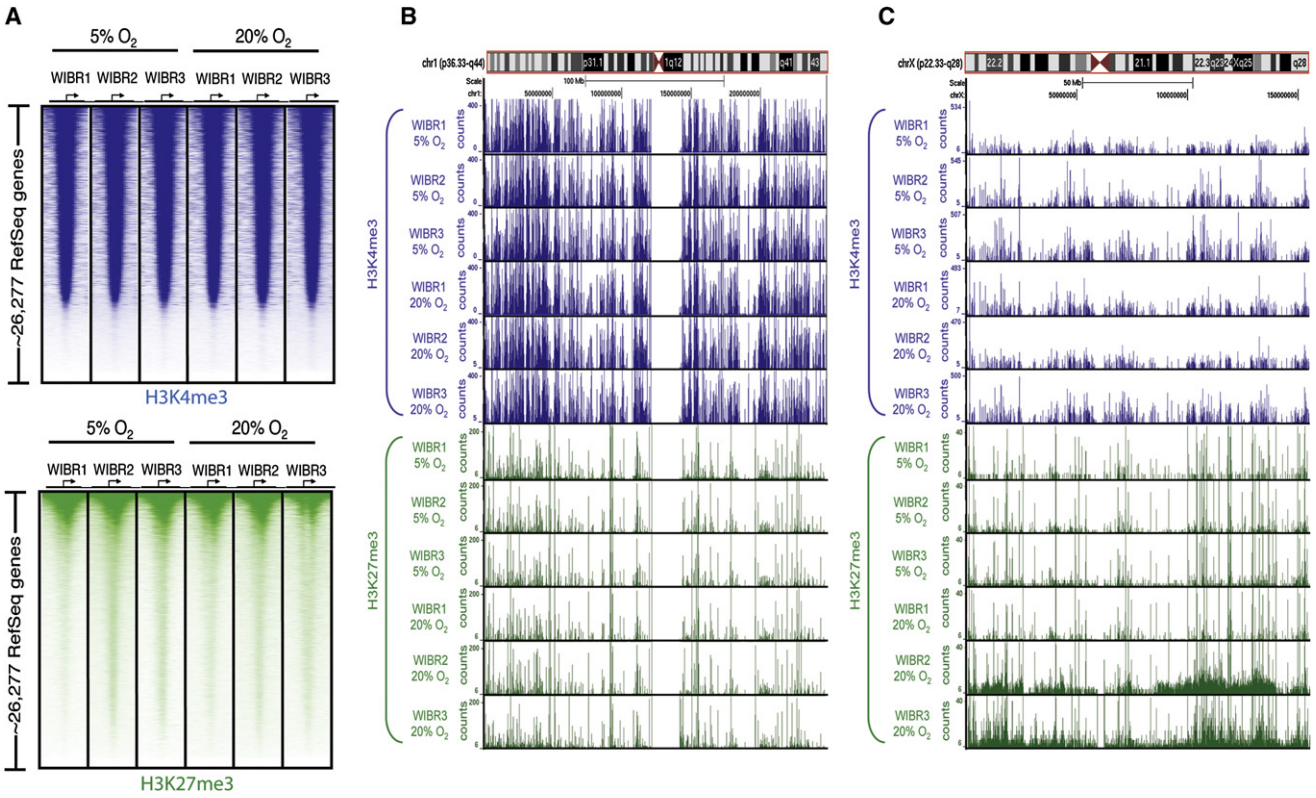

Figure 5. Localization of Activating and Repressive Histone Modifications

(A) ChIP-Seq profile of H3K4me3 (blue) and H3K27me3 (green) for all annotated human genes (26,277 RefSeq genes). The genomic region from −4 kb to +4 kb relative to the transcriptional start site is shown for each cell line and O_2 condition. Genes were ordered separately for H3K4me3 and H3K27me3 by the average ChIP-Seq density in 5% O_2 for WIBR1, 2, and 3 and arranged from highest to lowest density. An arrow indicates the start site and direction of transcription.

(B and C) ChIP-Seq profile of H3K4me3 (blue) and H3K27me3 (green) chromatin modifications along chromosome 1 (B) and the X chromosome (C) in the male hESC line WIBR1 and the female hESC lines WIBR2 and WIBR3. Chromosome maps and size scales are shown at the top of the graph.

able to suppress *XIST* expression, with several antioxidant-cultured cells exhibiting undetectable levels of *XIST* indistinguishable from the parental 5% O_2 cultures (Figure 4E). We confirmed the presence of XIST clouds in untreated 20% O_2 cultures and observed no XIST foci in the antioxidant treated cultures (Figure 4F), demonstrating that inhibition of oxidative stress is sufficient to protect hESCs from precocious XCI after exposure to atmospheric O_2.

Genome-wide Analysis of Histone Modifications

To correlate the activity of the X chromosome with the chromatin state in hESCs cultured in 20% or 5% O_2, we performed genome-wide location analysis of histone modifications that mark active (H3K4-me3) and repressed (H3K27-me3) genes. The distribution of these histone modifications on autosomes was grossly unaffected by changes in O_2 concentration (Figures 5A and 5B). We did, however, observe a dramatic accumulation of H3K27-me3 on the Xi of the female cell lines WIBR2$^{20\%}$ and WIBR3$^{20\%}$ (Figure 5C) that was not observed in the female hESC lines maintained under 5% O_2 or in the male hESC line WIBR1 in either O_2 environment. This is consistent with the observed monoallelic X-linked gene expression in female hESCs maintained in 20% O_2 and further supports the conclusion that these cells have undergone XCI. Thus, repressive histone modifications seem sufficient to maintain a level of gene silencing in line WIBR2$^{20\%}$ in the absence of XIST, as has previously been suggested (Shen et al., 2008; Zhang et al., 2007).

XCI Status in hESC Lines Derived from Cryopreserved Blastocysts

In addition to examining XCI in hESCs derived from embryos cultured in physiological O_2 prior to hESC derivation, we also determined the XCI state in several hESC lines derived from embryos cultured to the blastocyst stage under 20% O_2 and then cryopreserved. We thawed 12 cryopreserved blastocysts and allowed the blastocoels to expand (two blastocysts failed to expand; Table 1 and Table S1) prior to transferring them to 5% O_2. We obtained three additional hESC lines: two female (WIBR4 and WIBR5) and one male (WIBR6) (Figures S1 and S2). XIST FISH indicated that line WIBR4 was XaXa, while WIBR5 (derived from a blastocyst that failed to expand its blastocoel) had undergone X inactivation (Figure S6). This finding demonstrates that it is possible to isolate XaXa hESC lines from embryos frozen at the blastocyst stage, although the additional stress of this procedure may result in an increased probability of precocious XCI.

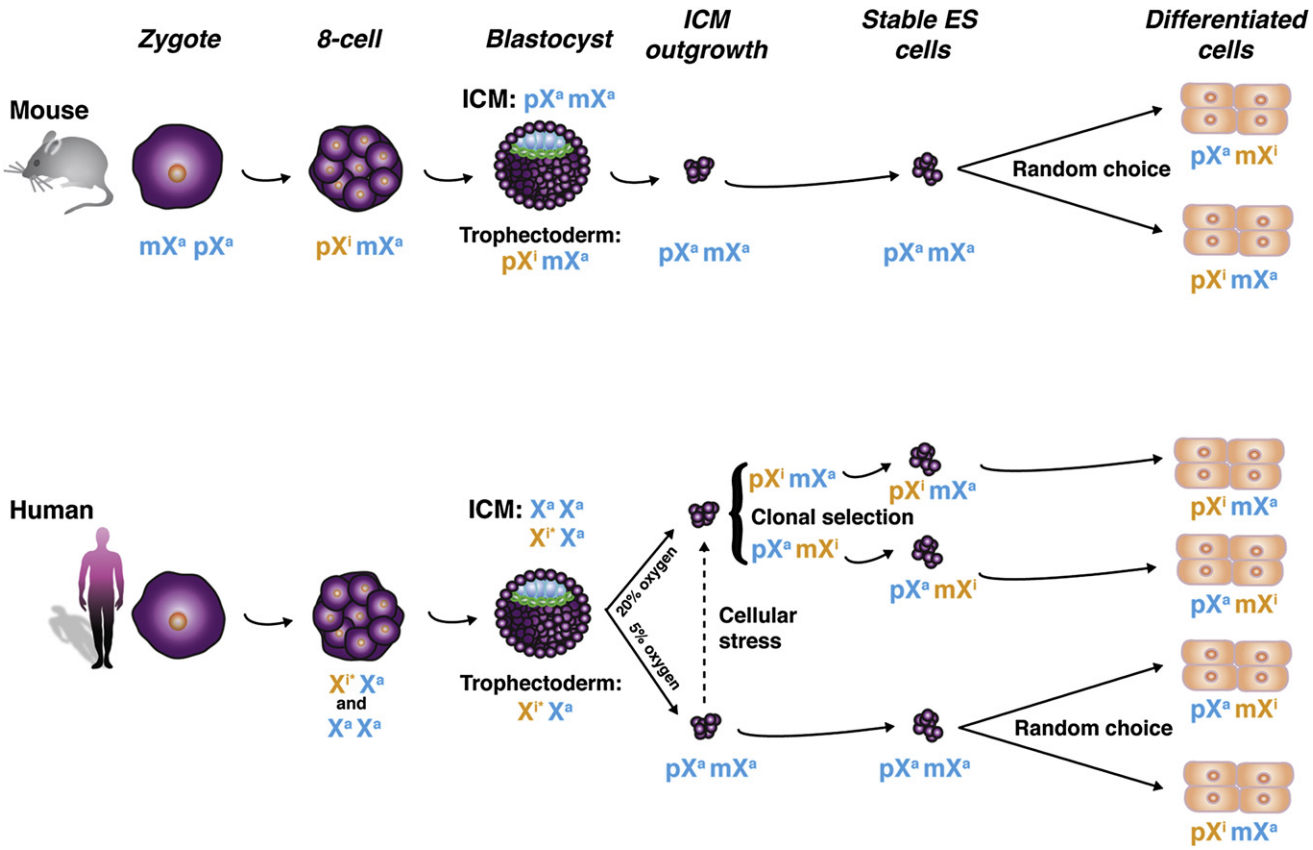

Figure 6. Model of XCI During Development and ESC Culture

Preimplantation mouse embryos exhibit imprinted silencing of the paternal chromosome (pXi) after the two-cell stage, which becomes reactivated in the ICM resulting in cells with two active X chromosomes (pXa mXa). Derivation of mouse ESCs results in XaXa cultures that undergo random XCI. In contrast, human preimplantation embryos contain cells both with and without XIST clouds. Derivation of XaXa hESCs from human blastocysts under physiological O_2 concentrations suggests the existence of XaXa cells in human blastocysts. Derivation of hESCs under atmospheric O_2 concentrations results in random XCI, after which prolonged in vitro culture results in clonal selection leading to monoallelic X-linked gene expression. hESCs maintained in physiological O_2 stably express both X chromosomes until encountering cellular stress or differentiation signals resulting in random XCI. X^{i*} in human preimplantation embryos indicates that although an XIST cloud is present, these cells have not been formally shown to have undergone silencing of the X chromosome.

DISCUSSION

Human ESCs differ in their propensity for spontaneous differentiation and X chromosome inactivation. The causes underlying this variability have been difficult to determine as a result of genetic heterogeneity between human ESCs, as well as variations in environmental and culture conditions. Here, we demonstrate that growth in atmospheric O_2 promotes XCI in three pairs of genetically identical hESC lines, while growth in physiological O_2 protects against promiscuous XCI.

In the mouse, the paternal X chromosome is imprinted and gradually becomes silenced sometime after the two-cell stage (Huynh and Lee, 2003; Kalantry et al., 2009; Okamoto et al., 2004; Patrat et al., 2009) (Figure 6). During blastocyst formation, cells of the ICM reactivate the Xi (Mak et al., 2004; Okamoto et al., 2004), and random X inactivation is initiated in the epiblast lineage upon implantation (Monkhorst et al., 2008; Payer and Lee, 2008). Establishment of murine ESCs from the ICM results in cultures that have reactivated the imprinted Xi and have biallelic X-linked gene expression (Mak et al., 2004; Okamoto et al., 2004; Wutz and Jaenisch, 2000), whereas derivation of EpiSCs from the postimplantation mouse epiblast results in cultures that have undergone random XCI as seen after differentiation (Guo et al., 2009).

Recent evidence suggests that a single XIST focus begins to form in each blastomere of six to eight cell human embryos (van den Berg et al., 2009), but it remained unknown whether cells of the blastocyst ICM reactivate this putative Xi. The observation that all hESC lines analyzed to date have undergone XCI in most or all cells has led to the idea that hESCs may correspond developmentally to murine EpiSCs rather than the pre-XCI, murine ESCs (Hall et al., 2008; Nichols and Smith, 2009; Shen et al., 2008; Silva et al., 2008). This is further supported by similarities in gene expression patterns, morphology and growth factor requirements of hESCs and murine EpiSCs. In the female hESC lines described in this study, those cultured in 20% O_2 exhibited XCI patterns consistent with what has been reported (either having XIST foci in most or all cells or having an inactive

X but lacking XIST foci and the ability to upregulate *XIST* upon differentiation). In contrast, hESC lines that were derived and maintained in 5% O_2 exhibited no XIST-positive cells even after prolonged culture and retained the ability to activate *XIST*, making them the first XaXa hESC lines isolated to date.

Using XaXa hESCs cultured at 5% O_2, we demonstrate that exposure to atmospheric O_2 alone is sufficient to initiate irreversible XCI. We also show that XCI can be prevented by treating hESC cultures with antioxidants, and, conversely, that induction of XCI is not limited to oxidative stress but occurs in response to other types of cellular stress. These findings suggest that in hESCs, XCI is governed by the cellular stress response. Furthermore, we demonstrate that in the XaXa state where the *XIST* gene is silent, the *XIST* promoter is heavily methylated, and, upon XCI, one *XIST* allele becomes demethylated, consistent with monoallelic *XIST* gene activation. Thus, the *XIST* gene in undifferentiated hESCs is fully methylated and not expressed, unlike the *Xist* gene in murine ESCs, which is expressed at low levels and only partially methylated (Nesterova et al., 2008; Sun et al., 2006).

Since hESC lines WIBR2$^{20\%}$ and WIBR3$^{20\%}$ underwent XCI during the culture period and exhibited monoallelic expression of X-linked genes similar to what has been reported in established hESC lines (Shen et al., 2008), it was important to address whether the monoallelic X-linked gene expression represented a nonrandom XCI event such as the paternally imprinted XCI that occurs in preimplantation murine development, or whether the cells underwent random XCI followed by selective clonal expansion of hESCs with one particular Xi. We utilized the ability of WIBR3$^{5\%}$ to undergo XCI to address this question, and we found that hESCs undergo random XCI upon differentiation, supporting the notion that the monoallelic expression in WIBR2$^{20\%}$ and WIBR3$^{20\%}$ is the result of clonal selection rather than imprinted XCI (Figure 6). Our data suggest that the conventional method of hESC isolation under atmospheric O_2 conditions not only induces precocious XCI but also imposes cellular stress leading to proliferation of some cells, perhaps those best adapted to the suboptimal growth conditions. This eventually may favor outgrowth of a few cells, leading to oligoclonal and ultimately monoclonal cultures with the same parental X inactivated in all cells and resulting in monoclonal X-linked gene expression, as suggested previously (Shen et al., 2008).

Monoallelic expression in WIBR2$^{20\%}$ in the absence of XIST coating the Xi after prolonged culture is consistent with previous data demonstrating that *XIST* activity, while necessary for initiation, is not required for maintaining the inactive state (Wutz et al., 2002). Indeed, WIBR2$^{20\%}$ had repressive histone H3K27-me3 coating the Xi in cells that displayed XIST clouds during early passages but were devoid of XIST at later passages, suggesting that H3K27-me3 may be sufficient to maintain the inactive state. This observation is in contrast to studies employing immunofluorescence to detect H3K27-me3 in mouse and human cells that found a direct correlation between the absence of XIST/Xist and H3K27-me3 foci (Shen et al., 2008; Zhang et al., 2007). This discrepancy is likely due to the relative insensitivity of immunofluorescence (where a large H3K27-me3 focus on the Xi is required for detection above autosomal staining) in comparison to the highly sensitive chromatin immunoprecipitation-based sequencing (ChIP-Seq) technique employed in this study.

The derivation of XaXa hESCs strongly suggests that cells in the ICM of human blastocysts, like those of the mouse, exist in the pre-XCI state. In a recent study, cells with XIST foci were detected in human blastocysts, suggesting that XCI has already occurred at this stage (van den Berg et al., 2009). However, on based on the location of the XIST-positive cells at the outer edges of the blastocyst, it is likely that these cells are of trophectodermal lineage and not pluripotent cells of the ICM.

In summary, we demonstrate that exposure to atmospheric O_2 results in precocious XCI in hESCs, whereas derivation under physiological O_2, using traditional hESC media, permits the establishment of pre-XCI hESCs. Because hESCs isolated under 5% O_2 appear to better retain the "ground state" of pluripotency with two active X chromosomes, the system is uniquely suited for the study of XCI in hESCs as has traditionally been done in the mouse. In addition, our findings are relevant for efforts to induce pluripotent cells by direct reprogramming as it may be possible to generate iPS cells from somatic human cells that correspond to mouse iPS cells when cultured under physiological oxygen.

EXPERIMENTAL PROCEDURES

Embryo Culture and ICM Isolation

Human embryos at the eight-cell or blastocyst stage produced by in vitro fertilization for clinical purposes were obtained with written informed consent and approved by an MIT institutional review board. Embryos were thawed and cultured in Global medium (LifeGlobal, Guelph, Ontario, Canada) with 15% human plasmanate (Bayer, Leverkusen, Germany) until day 6 in 5% O_2, 3% CO_2. ICM isolation was carried out after removal of the zona pelucida in the presence or absence of immunosurgery. The isolated ICM was cultured on mitomycin C-inactivated MEF feeders, and cultures were split into 20% O_2 after the first passage. Detailed methodology regarding blastocyst grading and culture procedures can be found in the Extended Experimental Procedures. Teratoma analysis was performed as described (Soldner et al., 2009) and in the Extended Experimental Procedures.

Immunocytochemistry and Flow Cytometry

Cells were fixed in 4% paraformaldehyde and immunostained as previously described (Soldner et al., 2009). For flow cytometry, hESCs grown on GFP-expressing MEFs were isolated as described in the Extended Experimental Procedures and stained with an anti-SSEA4 antibody, or, for OCT4, cells were fixed/permeabilized with an intracellular staining kit (R&D systems, Minneapolis, MN) and stained with anti-OCT4 antibody (Santa Cruz C-10) followed by staining with Alexa 647 anti-mouse secondary antibody (1:100). Total human cells were analyzed by gating out GFP+ MEF feeders. Data was processed with FlowJo software.

Karyotype and Fingerprint Analysis

Karyotype analysis was performed by the Cell Line Genetics Laboratory (Madison, WI).

qRT-PCR and Microarray Analysis

RNA was isolated with Trizol (GIBCO, Invitrogen, Carlsbad, CA) according to the manufacturer's protocol and was subsequently treated with DNase I with an RNase free DNase kit (Zymo Research, Orange County, CA). Quantitative RT-PCR analysis was performed as described previously (Lengner et al., 2007) with primers described in the Extended Experimental Procedures. Microarray analysis and data processing was performed as described in the Extended Experimental Procedures, and raw data are available under the Gene Expression Omnibus (GEO) accession number GSE20937.

RNA/DNA FISH and Immunofluorescence

RNA and DNA FISH were carried out as described (Lee and Lu, 1999). Dispersed hESCs were cytospun onto glass slides prior to fixation. Complementary DNA (cDNA) probes were generated to *XIST* exon 1 (GenBank U80460: 61251–69449) and exon 6 (U80460: 75081–78658), labeled by nick translation (Roche, Indianapolis, IN) with Cy3-dUTP (Amersham), and Cot-1 DNA was labeled with fluoroscein-12-dUTP with a Prime-It Fluor Labeling kit (Stratagene, La Jolla, CA). After RNA FISH, 0.2 μm Z section images were captured, and the Z sections were merged. StarFISH X chromosomal paints (Cambio, Cambridge, UK) were hybridized according to the manufacturer's instructions. In sequential RNA/DNA FISH, RNA FISH was performed first, 0.2 μm Z section images were captured, and their x-y coordinates were marked, and then the same slide was denatured for DNA FISH. For X-linked gene FISH, a BAC containing the *TIMP1* genomic locus was labeled by nick translation with Cy3-dUTP, and hybridization/imaging was performed as for *XIST*. Images were overlaid using DAPI nuclear staining as a reference.

DNA Methylation Analysis

Conversion of DNA with sodium bisulfite was performed with the EZ-96 DNA Methylation Kit (Zymo Research, Orange County, CA) with 1 ug DNA and the alternative conversion protocol (two temperature DNA denaturation). Sequenom's MassARRAY platform was used to perform quantitative methylation analysis as described in the Extended Experimental Procedures, and manual bisulfite sequence analysis was performed as described (Soldner et al., 2009).

Allele-Specific Expression Analysis

X-linked gene expression analysis was performed on nuclear RNA as described (Gimelbrant et al., 2007). Sequenom genotyping was used for precise measurement of allelic imbalance in DNA and cDNA samples (see Cowles et al., 2002, and Gimelbrant and Chess, 2006, and references therein). This involves PCR amplification of a small region flanking the SNP of interest, followed by primer extension and mass spectrometry detection of extended species. Details of these analyses are described in the Extended Experimental Procedures.

Chromatin Immunoprecipitation and Sequencing

The antibodies for ChIP were specific for H3K4me3 (ab 8580) and H3K27me3 (ab 6002). Protocols describing materials and methods have been previously described (Lee et al., 2006), can be downloaded at http://web.wi.mit.edu/young/hES_PRC/, and are described in the Extended Experimental Procedures.

ACCESSION NUMBERS

The GEO accession number for the transcriptome profiling data reported in this paper is GSE20937. The GEO accession number for the ChIP-Sequencing data reported in this paper is GSE21141.

SUPPLEMENTAL INFORMATION

Supplemental Information includes Extended Experimental Procedures, seven figures, and three tables and can be found with this article online at doi:10.1016/j.cell.2010.04.010.

ACKNOWLEDGMENTS

We thank J. Dausman for animal husbandry; F. Soldner and B. Zhou for useful discussions and technical assistance with hESC culture and FACS analysis of hESCs; J. Kwon, J. Love, T. Volkert, and S. Gupta at the WIBR Genome Technology Core for microarray processing; D.D. Fu and Q. Gao for teratoma processing/analysis; P. Shaw for Sequenom methylation analysis; C. Larkin and R. Holmes for assistance with IVF embryos; and members of the Jaenisch and Lee labs for fruitful discussions. We especially thank Hillel and Liliana Bachrach and Susan Whitehead for their generous gifts enabling this research. R.J. is cofounder of Fate Therapeutics and adviser to Stemgent.

Received: October 29, 2009
Revised: February 11, 2010
Accepted: April 1, 2010
Published online: May 13, 2010

REFERENCES

Batt, P.A., Gardner, D.K., and Cameron, A.W. (1991). Oxygen concentration and protein source affect the development of preimplantation goat embryos in vitro. Reprod. Fertil. Dev. *3*, 601–607.

Bernardi, M.L., Fléchon, J.E., and Delouis, C. (1996). Influence of culture system and oxygen tension on the development of ovine zygotes matured and fertilized in vitro. J. Reprod. Fertil. *106*, 161–167.

Boggs, B.A., Cheung, P., Heard, E., Spector, D.L., Chinault, A.C., and Allis, C.D. (2002). Differentially methylated forms of histone H3 show unique association patterns with inactive human X chromosomes. Nat. Genet. *30*, 73–76.

Brons, I.G., Smithers, L.E., Trotter, M.W., Rugg-Gunn, P., Sun, B., Chuva de Sousa Lopes, S.M., Howlett, S.K., Clarkson, A., Ahrlund-Richter, L., Pedersen, R.A., and Vallier, L. (2007). Derivation of pluripotent epiblast stem cells from mammalian embryos. Nature *448*, 191–195.

Chen, H.F., Kuo, H.C., Chen, W., Wu, F.C., Yang, Y.S., and Ho, H.N. (2009). A reduced oxygen tension (5%) is not beneficial for maintaining human embryonic stem cells in the undifferentiated state with short splitting intervals. Hum. Reprod. *24*, 71–80.

Cowan, C.A., Klimanskaya, I., McMahon, J., Atienza, J., Witmyer, J., Zucker, J.P., Wang, S., Morton, C.C., McMahon, A.P., Powers, D., and Melton, D.A. (2004). Derivation of embryonic stem-cell lines from human blastocysts. N. Engl. J. Med. *350*, 1353–1356.

Cowles, C.R., Hirschhorn, J.N., Altshuler, D., and Lander, E.S. (2002). Detection of regulatory variation in mouse genes. Nat. Genet. *32*, 432–437.

Ezashi, T., Das, P., and Roberts, R.M. (2005). Low O2 tensions and the prevention of differentiation of hES cells. Proc. Natl. Acad. Sci. USA *102*, 4783–4788.

Fischer, B., and Bavister, B.D. (1993). Oxygen tension in the oviduct and uterus of rhesus monkeys, hamsters and rabbits. J. Reprod. Fertil. *99*, 673–679.

Forsyth, N.R., Musio, A., Vezzoni, P., Simpson, A.H., Noble, B.S., and McWhir, J. (2006). Physiologic oxygen enhances human embryonic stem cell clonal recovery and reduces chromosomal abnormalities. Cloning Stem Cells *8*, 16–23.

Forsyth, N.R., Kay, A., Hampson, K., Downing, A., Talbot, R., and McWhir, J. (2008). Transcriptome alterations due to physiological normoxic (2% O2) culture of human embryonic stem cells. Regen. Med. *3*, 817–833.

Gimelbrant, A.A., and Chess, A. (2006). An epigenetic state associated with areas of gene duplication. Genome Res. *16*, 723–729.

Gimelbrant, A., Hutchinson, J.N., Thompson, B.R., and Chess, A. (2007). Widespread monoallelic expression on human autosomes. Science *318*, 1136–1140.

Guo, G., Yang, J., Nichols, J., Hall, J.S., Eyres, I., Mansfield, W., and Smith, A. (2009). Klf4 reverts developmentally programmed restriction of ground state pluripotency. Development *136*, 1063–1069.

Hall, L.L., Byron, M., Butler, J., Becker, K.A., Nelson, A., Amit, M., Itskovitz-Eldor, J., Stein, J., Stein, G., Ware, C., and Lawrence, J.B. (2008). X-inactivation reveals epigenetic anomalies in most hESC but identifies sublines that initiate as expected. J. Cell. Physiol. *216*, 445–452.

Harlow, G.M., and Quinn, P. (1979). Foetal and placental growth in the mouse after pre-implantation development in vitro under oxygen concentrations of 5 and 20%. Aust. J. Biol. Sci. *32*, 363–369.

Heard, E., Rougeulle, C., Arnaud, D., Avner, P., Allis, C.D., and Spector, D.L. (2001). Methylation of histone H3 at Lys-9 is an early mark on the X chromosome during X inactivation. Cell *107*, 727–738.

Huynh, K.D., and Lee, J.T. (2003). Inheritance of a pre-inactivated paternal X chromosome in early mouse embryos. Nature *426*, 857–862.

Kalantry, S., Purushothaman, S., Bowen, R.B., Starmer, J., and Magnuson, T. (2009). Evidence of Xist RNA-independent initiation of mouse imprinted X-chromosome inactivation. Nature *460*, 647–651.

Karja, N.W., Wongsrikeao, P., Murakami, M., Agung, B., Fahrudin, M., Nagai, T., and Otoi, T. (2004). Effects of oxygen tension on the development and quality of porcine in vitro fertilized embryos. Theriogenology *62*, 1585–1595.

Kay, G.F., Penny, G.D., Patel, D., Ashworth, A., Brockdorff, N., and Rastan, S. (1993). Expression of Xist during mouse development suggests a role in the initiation of X chromosome inactivation. Cell *72*, 171–182.

Kikuchi, K., Onishi, A., Kashiwazaki, N., Iwamoto, M., Noguchi, J., Kaneko, H., Akita, T., and Nagai, T. (2002). Successful piglet production after transfer of blastocysts produced by a modified in vitro system. Biol. Reprod. *66*, 1033–1041.

Kitagawa, Y., Suzuki, K., Yoneda, A., and Watanabe, T. (2004). Effects of oxygen concentration and antioxidants on the in vitro developmental ability, production of reactive oxygen species (ROS), and DNA fragmentation in porcine embryos. Theriogenology *62*, 1186–1197.

Kohlmaier, A., Savarese, F., Lachner, M., Martens, J., Jenuwein, T., and Wutz, A. (2004). A chromosomal memory triggered by Xist regulates histone methylation in X inactivation. PLoS Biol. *2*, E171.

Lee, J.T., and Lu, N. (1999). Targeted mutagenesis of Tsix leads to nonrandom X inactivation. Cell *99*, 47–57.

Lee, T.I., Johnstone, S.E., and Young, R.A. (2006). Chromatin immunoprecipitation and microarray-based analysis of protein location. Nat. Protoc. *1*, 729–748.

Lengner, C.J., Camargo, F.D., Hochedlinger, K., Welstead, G.G., Zaidi, S., Gokhale, S., Scholer, H.R., Tomilin, A., and Jaenisch, R. (2007). Oct4 expression is not required for mouse somatic stem cell self-renewal. Cell Stem Cell *1*, 403–415.

Ludwig, T.E., Levenstein, M.E., Jones, J.M., Berggren, W.T., Mitchen, E.R., Frane, J.L., Crandall, L.J., Daigh, C.A., Conard, K.R., Piekarczyk, M.S., et al. (2006). Derivation of human embryonic stem cells in defined conditions. Nat. Biotechnol. *24*, 185–187.

Mak, W., Nesterova, T.B., de Napoles, M., Appanah, R., Yamanaka, S., Otte, A.P., and Brockdorff, N. (2004). Reactivation of the paternal X chromosome in early mouse embryos. Science *303*, 666–669.

Mermoud, J.E., Popova, B., Peters, A.H., Jenuwein, T., and Brockdorff, N. (2002). Histone H3 lysine 9 methylation occurs rapidly at the onset of random X chromosome inactivation. Curr. Biol. *12*, 247–251.

Monkhorst, K., Jonkers, I., Rentmeester, E., Grosveld, F., and Gribnau, J. (2008). X inactivation counting and choice is a stochastic process: evidence for involvement of an X-linked activator. Cell *132*, 410–421.

Nesterova, T.B., Popova, B.C., Cobb, B.S., Norton, S., Senner, C.E., Tang, Y.A., Spruce, T., Rodriguez, T.A., Sado, T., Merkenschlager, M., and Brockdorff, N. (2008). Dicer regulates Xist promoter methylation in ES cells indirectly through transcriptional control of Dnmt3a. Epigenetics Chromatin *1*, 2.

Nichols, J., and Smith, A. (2009). Naive and primed pluripotent states. Cell Stem Cell *4*, 487–492.

Okamoto, I., Otte, A.P., Allis, C.D., Reinberg, D., and Heard, E. (2004). Epigenetic dynamics of imprinted X inactivation during early mouse development. Science *303*, 644–649.

Panning, B., Dausman, J., and Jaenisch, R. (1997). X chromosome inactivation is mediated by Xist RNA stabilization. Cell *90*, 907–916.

Parrinello, S., Samper, E., Krtolica, A., Goldstein, J., Melov, S., and Campisi, J. (2003). Oxygen sensitivity severely limits the replicative lifespan of murine fibroblasts. Nat. Cell Biol. *5*, 741–747.

Patrat, C., Okamoto, I., Diabangouaya, P., Vialon, V., Le Baccon, P., Chow, J., and Heard, E. (2009). Dynamic changes in paternal X-chromosome activity during imprinted X-chromosome inactivation in mice. Proc. Natl. Acad. Sci. USA *106*, 5198–5203.

Payer, B., and Lee, J.T. (2008). X chromosome dosage compensation: how mammals keep the balance. Annu. Rev. Genet. *42*, 733–772.

Penny, G.D., Kay, G.F., Sheardown, S.A., Rastan, S., and Brockdorff, N. (1996). Requirement for Xist in X chromosome inactivation. Nature *379*, 131–137.

Plath, K., Fang, J., Mlynarczyk-Evans, S.K., Cao, R., Worringer, K.A., Wang, H., de la Cruz, C.C., Otte, A.P., Panning, B., and Zhang, Y. (2003). Role of histone H3 lysine 27 methylation in X inactivation. Science *300*, 131–135.

Prasad, S.M., Czepiel, M., Cetinkaya, C., Smigielska, K., Weli, S.C., Lysdahl, H., Gabrielsen, A., Petersen, K., Ehlers, N., Fink, T., et al. (2009). Continuous hypoxic culturing maintains activation of Notch and allows long-term propagation of human embryonic stem cells without spontaneous differentiation. Cell Prolif. *42*, 63–74.

Quinn, P., and Harlow, G.M. (1978). The effect of oxygen on the development of preimplantation mouse embryos in vitro. J. Exp. Zool. *206*, 73–80.

Reubinoff, B.E., Pera, M.F., Fong, C.Y., Trounson, A., and Bongso, A. (2000). Embryonic stem cell lines from human blastocysts: somatic differentiation in vitro. Nat. Biotechnol. *18*, 399–404.

Shen, Y., Matsuno, Y., Fouse, S.D., Rao, N., Root, S., Xu, R., Pellegrini, M., Riggs, A.D., and Fan, G. (2008). X-inactivation in female human embryonic stem cells is in a nonrandom pattern and prone to epigenetic alterations. Proc. Natl. Acad. Sci. USA *105*, 4709–4714.

Silva, S.S., Rowntree, R.K., Mekhoubad, S., and Lee, J.T. (2008). X-chromosome inactivation and epigenetic fluidity in human embryonic stem cells. Proc. Natl. Acad. Sci. USA *105*, 4820–4825.

Soldner, F., Hockemeyer, D., Beard, C., Gao, Q., Bell, G.W., Cook, E.G., Hargus, G., Blak, A., Cooper, O., Mitalipova, M., et al. (2009). Parkinson's disease patient-derived induced pluripotent stem cells free of viral reprogramming factors. Cell *136*, 964–977.

Sun, B.K., Deaton, A.M., and Lee, J.T. (2006). A transient heterochromatic state in Xist preempts X inactivation choice without RNA stabilization. Mol. Cell *21*, 617–628.

Tesar, P.J., Chenoweth, J.G., Brook, F.A., Davies, T.J., Evans, E.P., Mack, D.L., Gardner, R.L., and McKay, R.D. (2007). New cell lines from mouse epiblast share defining features with human embryonic stem cells. Nature *448*, 196–199.

Thompson, J.G., Simpson, A.C., Pugh, P.A., Donnelly, P.E., and Tervit, H.R. (1990). Effect of oxygen concentration on in-vitro development of preimplantation sheep and cattle embryos. J. Reprod. Fertil. *89*, 573–578.

Thomson, J.A., Itskovitz-Eldor, J., Shapiro, S.S., Waknitz, M.A., Swiergiel, J.J., Marshall, V.S., and Jones, J.M. (1998). Embryonic stem cell lines derived from human blastocysts. Science *282*, 1145–1147.

van den Berg, I.M., Laven, J.S., Stevens, M., Jonkers, I., Galjaard, R.J., Gribnau, J., and van Doorninck, J.H. (2009). X chromosome inactivation is initiated in human preimplantation embryos. Am. J. Hum. Genet. *84*, 771–779.

Wang, F., Thirumangalathu, S., and Loeken, M.R. (2006). Establishment of new mouse embryonic stem cell lines is improved by physiological glucose and oxygen. Cloning Stem Cells *8*, 108–116.

Ware, C.B., Wang, L., Mecham, B.H., Shen, L., Nelson, A.M., Bar, M., Lamba, D.A., Dauphin, D.S., Buckingham, B., Askari, B., et al. (2009). Histone deacetylase inhibition elicits an evolutionarily conserved self-renewal program in embryonic stem cells. Cell Stem Cell *4*, 359–369.

Wutz, A., and Jaenisch, R. (2000). A shift from reversible to irreversible X inactivation is triggered during ES cell differentiation. Mol. Cell *5*, 695–705.

Wutz, A., Rasmussen, T.P., and Jaenisch, R. (2002). Chromosomal silencing and localization are mediated by different domains of Xist RNA. Nat. Genet. *30*, 167–174.

Yoshida, Y., Takahashi, K., Okita, K., Ichisaka, T., and Yamanaka, S. (2009). Hypoxia enhances the generation of induced pluripotent stem cells. Cell Stem Cell *5*, 237–241.

Zhang, L.F., Huynh, K.D., and Lee, J.T. (2007). Perinucleolar targeting of the inactive X during S phase: evidence for a role in the maintenance of silencing. Cell *129*, 693–706.